

# Crestal Bone Changes Around Titanium Implants: A Methodologic Study Comparing Linear Radiographic with Histometric Measurements

Joachim S. Hermann, DMD, Dr Med Dent, FICOI<sup>1</sup>/John D. Schoolfield, MS<sup>2</sup>/

Pirkka V. Nummikoski, DDS, MS<sup>3</sup>/Daniel Buser, DMD, Prof Dr Med Dent<sup>4</sup>/

Robert K. Schenk, MD, Prof Dr Med<sup>5</sup>/David L. Cochran, DDS, PhD, MS, MMSci, FACD, FICD<sup>6</sup>

Generally, endosseous implants can be placed according to a nonsubmerged or a submerged technique and in 1-piece or 2-piece configurations. Recently, it has been shown that peri-implant crestal bone reactions differ significantly radiographically as well as histometrically under such conditions and are dependent on a rough/smooth implant border in 1-piece implants and on the location of a microgap (interface) between the implant and the abutment/restoration in 2-piece configurations. The purpose of this study was to evaluate whether standardized radiography as a noninvasive clinical diagnostic method correlates with peri-implant crestal bone levels as determined by histometric analysis. Fifty-nine implants were placed in edentulous mandibular areas of 5 foxhounds in a side-by-side comparison in both submerged and nonsubmerged techniques. Three months after implant placement, abutment connection was performed in the submerged implant sites. At 6 months, all animals were sacrificed, and evaluations of the first bone-to-implant contact (fBIC), determined on standardized periapical radiographs, were compared to similar analyses made from nondecalcified histology. It was shown that both techniques provide the same information (Pearson correlation coefficient = 0.993;  $P < .001$ ). The precision of the radiographs was within 0.1 mm of the histometry in 73.4% of the evaluations, while the level of agreement fell to between 0.1 and 0.2 mm in 15.9% of the cases. These data demonstrate in an experimental study that standardized periapical radiography can evaluate crestal bone levels around implants clinically accurately (within 0.2 mm) in a high percentage (89%) of cases. These findings are significant because crestal bone levels can be determined using a noninvasive technique, and block sectioning or sacrifice of the animal subject is not required. In addition, longitudinal evaluations can be made accurately such that bone changes over various time periods can be assessed. Such analyses may prove beneficial when trying to distinguish physiologic changes from pathologic changes or when trying to determine causes and effects of bone changes around dental implants. (INT J ORAL MAXILLOFAC IMPLANTS 2001;16:475–485)

**Key words:** animal study, crestal bone loss, endosseous implants, histometry, standardized radiography

<sup>1</sup>Clinical Assistant Professor, Department of Periodontics, Dental School, University of Texas Health Science Center at San Antonio (UTHSCSA), Texas; Associate Professor, Head, and Postgraduate Program Director, Division of Periodontics, Department of Preventive Dentistry, Periodontics, and Cariology, University of Zürich Dental School, Zürich, Switzerland.

<sup>2</sup>Programmer Analyst III, Statistical/Mathematical Consulting, Computing Resources, UTHSCSA, Texas.

<sup>3</sup>Associate Professor, Department of Dental Diagnostic Science, UTHSCSA, Texas.

<sup>4</sup>Professor and Chairman, Department of Oral Surgery, University of Bern School of Dental Medicine, Bern, Switzerland.

<sup>5</sup>Professor Emeritus, Department of Oral Surgery, University of Bern School of Dental Medicine, Bern, Switzerland.

<sup>6</sup>Professor and Chairman, Department of Periodontics, Dental School, UTHSCSA Texas.

**Reprint requests:** David L. Cochran, UTHSCSA, Dental School, Department of Periodontics, 7703 Floyd Curl Drive, San Antonio, TX 78284-7894. Fax: (210) 567-3643. E-mail: Cochran@uthscsa.edu

Periodontitis<sup>1</sup> and peri-implantitis,<sup>2</sup> among other signs and symptoms, are associated with crestal bone loss. In an attempt to diagnose bone loss in inflammatory conditions as soon as possible and to possibly prevent further bone loss from occurring, reliable diagnostic methods are required. In addition, biologic principles governing crestal bone levels around dental implants facilitate a distinction between a physiologic degree of crestal bone remodeling and a pathologic condition resulting in continuing or more advanced peri-implant crestal bone loss. The accumulated evidence from side-by-side comparisons of different implant designs demonstrated that under healthy conditions, crestal bone levels significantly remodel apically for 2-piece implant designs dependent on the location of the

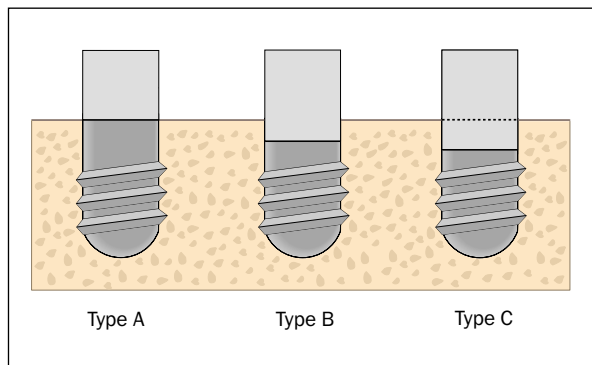


**Fig 1a** Schematic (true to scale) of implant types A, B, and C at time of implant placement in relation to the crestal bone level. The solid black line delineates the border between rough and smooth implant surfaces, whereas the dashed line shows the location of the microgap (interface) where appropriate. Note that types A to C were placed using a nonsubmerged approach. Implant types A and B are 1-piece implants exhibiting no microgap (interface), while type C implants are 2-piece implants with a microgap (interface) located at the crest of the bone. Reprinted from Hermann et al<sup>5</sup> with permission.

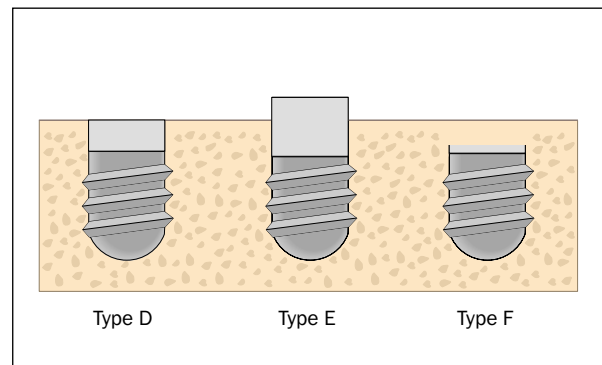


**Fig 1b** Schematic (true to scale) of implant types D, E, and F at the time of implant placement in relation to the crestal bone level. Note that these implants were placed using a submerged technique. Implant types D to F are 2-piece implants with a microgap (interface) located at different levels in relation to the crest of the bone. Reprinted from Hermann et al<sup>5</sup> with permission.

microgap ([MG]/interface [IF]), while minimal to no such resorption occurs for 1-piece implants, dependent on the location of a rough/smooth border and its relation to the original bone crest level.<sup>3-7</sup>

Radiography has been widely used during the last century as a noninvasive diagnostic method to help define whether loss of alveolar bone has occurred around teeth and/or implants. Early on, the bisecting angle technique for taking radiographs was introduced<sup>8</sup> as a freehand technique that is still in use as of today. A major problem involved with this technique, however, is a significant degree of distortion because of disproportional shrinkage or enlargement of the radiographically imaged tooth. This distortion then creates problems in the evaluation of small changes in the level of the bony crest. In the late 1950s, Benkow<sup>9,10</sup> suggested for the first time the use of a beam-aiming device made up of a bite block connected to an indicator arm, which itself was attached to a beam-aiming ring. Thus, projection errors could be decreased to a significant extent. Through this setup, the plane of the film (attached to the bite block) and the plane of the x-ray beams were perpendicular to each other (right-angle technique). However, this did not automatically allow alignment of the plane of the film parallel to the long axis of the tooth (paralleling technique). With the advent of beam-aiming devices rigidly connected to an intraoral radiographic template,<sup>11</sup> projection errors related to rotation and angulation could be further decreased by using a right-angle technique;

however, this was still in combination with a short x-ray cone and a more or less parallel orientation of the film to the long axis of the tooth. As a further development, Larheim and Eggen<sup>12</sup> showed for the first time in implant dentistry that standardized periapical radiography can be significantly improved if a customized bite record is additionally used in combination with a bite block and a long-cone technique.

The purpose of this study was to combine these techniques and to develop an improved standardized radiographic technique that would allow a precise determination of peri-implant crestal bone levels. Since conventional periapical radiography always represents cumulative data of the whole width of the jaw with potential under- and/or overestimation of true crestal bone levels,<sup>13-18</sup> the radiographic data were compared to histologic evaluations of identical bone levels.

## MATERIALS AND METHODS

Implant design and surfaces (Figs 1a and 1b), animals and surgical procedures/study design used in this study (Fig 2), and a detailed description of the radiographic and histologic analyses utilized (Fig 3) have been published recently.<sup>4,5</sup> Briefly, study protocols were as follows. Six different cylindrical titanium implants (A to F) with a full-body screw design were chosen (Figs 1a and 1b). All were made from cold-worked, grade IV commercially pure titanium (Insti-

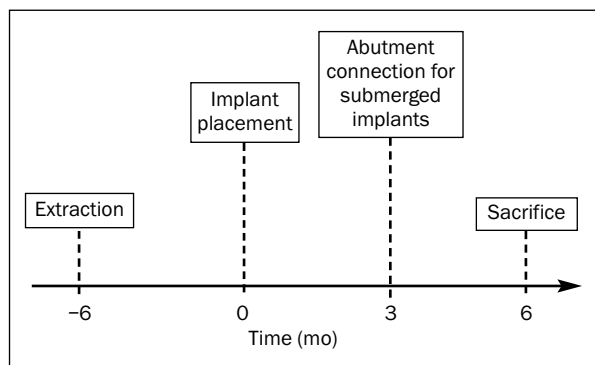
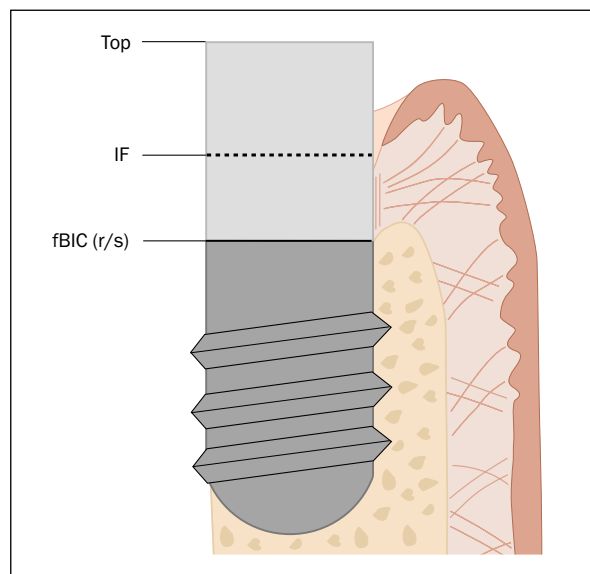


**Fig 2** (Above) Study design.

**Fig 3** (Right) Composite schematic (not true to scale) of radiographic/histometric evaluation with the following measurements: Distance from the top of the implant (types A and B) or the interface/microgap (IF; types C to F), respectively, to the first bone-to-implant contact (fBIC) as well as the rough/smooth border (r/s; histometry). Reprinted from Hermann et al<sup>5</sup> with permission.



tut Straumann AG, Waldenburg, Switzerland). The total length was 9 mm, and the outer diameter measured 4.1 mm. All implants had a relatively smooth coronal portion consisting of a machined titanium surface. The rough apical part of each implant had a sandblasted (large-grit) and hydrochloric acid/sulfuric acid- (HCl/H<sub>2</sub>SO<sub>4</sub>) etched surface (SLA) exhibiting 2 levels of roughness, one at 20 to 40  $\mu$ m peak to peak, and a superimposed second level at 2 to 4  $\mu$ m peak to peak. For type A implants, the SLA surface was 6.0 mm in length, with the rough/smooth implant border at the alveolar crest. For all other implants (types B to F), the rough implant surface (SLA) was 4.5 mm in vertical dimension, with the rough/smooth implant border located 1.5 mm below the crest. Type A and B implants were 1-piece implants, meaning there was no microgap (IF) present. Implant types C to F consisted of 2 pieces, with a microgap (IF) of about 50  $\mu$ m between the implant and the secondary component, the abutment (Fig 3). The location of the microgap (IF) was defined to be at the bone crest level for types C and D; for types E and F, the microgap (IF) was located 1 mm above and 1 mm below the crest, respectively. Implant types A to C were placed according to a nonsubmerged technique, whereas types D to F were placed using a submerged approach.

Five lab-bred, male American foxhounds (approximately 2 years old, weighing 30 to 35 kg) were used for this study. All procedures were approved by the Institutional Animal Care and Use

Committee of the University of Texas Health Science Center at San Antonio. First, all 4 premolars (P1–P4) and the first molar (M1) were extracted. After a period of 7 to 10 days, the sutures were removed. After a healing period of 6 months, non-submerged and submerged implants (types A to F) were placed (Fig 2). Implant types A to C were placed according to a nonsubmerged approach (Fig 1a), and implant types D to F were placed according to a submerged technique (Fig 1b). Finally, 1 of each kind of test implant was placed per side in a randomized fashion. Thus, no implant type had a biased position in the arch. Sutures were removed 7 to 10 days later.

Second-stage surgery was performed 3 months after implant placement (Fig 2), and abutments were connected for submerged implant types D to F. Abutments on all 2-piece implants (types C to F) were loosened and immediately tightened afterward at 4, 8, and 10 weeks after second-stage surgery to imitate the placement of another healing abutment, impression taking, and the placement of the final prosthetic component.

All dogs were sacrificed 3 months after abutment connection of the submerged implants or 6 months after implant placement, respectively (Fig 2). Mandibles were block-resected with an oscillating autopsy saw (Stryker, Kalamazoo, MI). The recovered segments with the implants were immersed in a solution of formaldehyde 4% combined with calcium chloride 1% for histologic preparation and analysis.

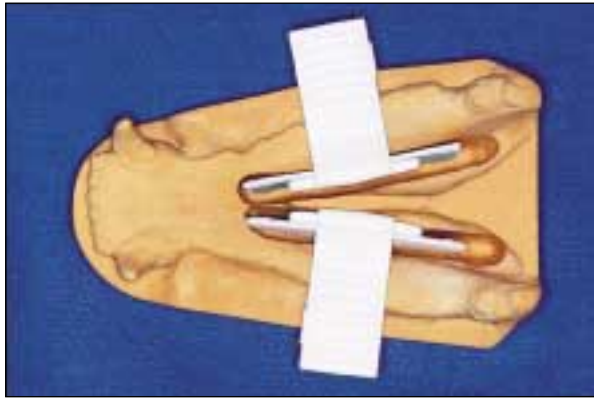


**Fig 4** Occlusal view of the cast of the partially edentulous canine mandible with radiographic bite blocks and mounted x-ray films in situ. Grooves were made on either side of the mandible lingually (soft mouth floor area) to allow for an ideal position of the radiograph, resulting in an optimum parallel and perpendicular technique.



**Fig 5** Lateral view of the complete radiographic template mounted on the cast and firmly fixed with a reversible adhesive tape.



**Fig 6** Anterior view of the complete radiographic template mounted on the cast and fixed with a reversible adhesive tape. Indicator arms were inserted into the holes of the bite blocks and thus rigidly connected to the x-ray beam-aiming device. Note that, in addition, the ring of the beam-aiming device was customized with acrylic resin material for better and more reproducible fit and alignment of the extension x-ray cone to minimize errors of angulation and distortion.

### Fabrication of the Radiographic Template

At the time of implant placement, an individual impression was made (President, Coltène/Whaledent, Mahwah, NJ) using customized trays fabricated from light-polymerizing acrylic resin material (Triad, Dentsply International, York, PA). A master cast (Fig 4) was made using die stone (Silky-Rock, Whip-Mix, Louisville, KY). Grooves were made on the lingual side of each edentulous ridge (soft mouth floor area), allowing accurate positioning of the periapical radiograph (Ultra-speed film, size 3, Eastman-Kodak, Rochester, NY) mounted on an x-ray bite block (XCP, Rinn, Dentsply International). The two ideally placed bite blocks were rigidly connected through a

horseshoe-shaped acrylic resin bar (Instant Tray Mix, Lang Dental, Wheeling, IL) and individual acrylic resin inverse U-shaped attachments (Triad, Dentsply International; Fig 5), providing space for a tape for final fixation. At both the mesial and distal ends of either side, customized soft polyvinyl siloxane records (President) from the cusps of the canine and second molar, respectively, were attached to the acrylic resin bar to allow for precise repositioning and stabilization of the radiographic template. A reversible adhesive tape (Velcro Tape, Velcro USA, Manchester, NH) was used to firmly attach the template to the dog's mandible (Figs 5 and 6). Finally, the ring of the beam-aiming devices was customized with some autopolymerizing acrylic resin material (Instant Tray Mix, Lang Dental) for an even better and more reproducible fit and alignment of the long x-ray cone (Fig 6). Thus, an optimum parallel and perpendicular standardized radiographic technique was possible for minimizing errors of angulation and distortion.

### Statistical Analysis

The distance from the top of the implant (Fig 3) to the first bone-to-implant contact (fBIC) was evaluated by examining mesial and distal sites in 59 implants using both standardized radiographs and histologic sections (Figs 7 to 10; Tables 1 and 2). Two implants had undetectable fBIC for both the mesial and the distal sites, and 1 implant had a readable fBIC for the mesial site only, resulting in a total of 113 sites for which the distance of Top-fBIC could be observed. Pearson correlation and least-squares regression were used to determine how closely the distances measured using standardized radiographs corresponded to the dimensions observed using

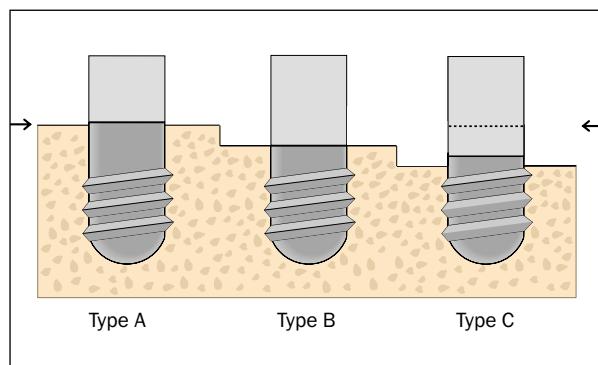


**Fig 7a** Histometric results: schematic (true to scale) of hard tissues around nonsubmerged implants types A to C at the time of sacrifice in relation to the rough/smooth border (solid black line) or the location of the microgap/interface (dashed black line) where appropriate. Arrows indicate the level of the crest of the bone at the time of implant placement.

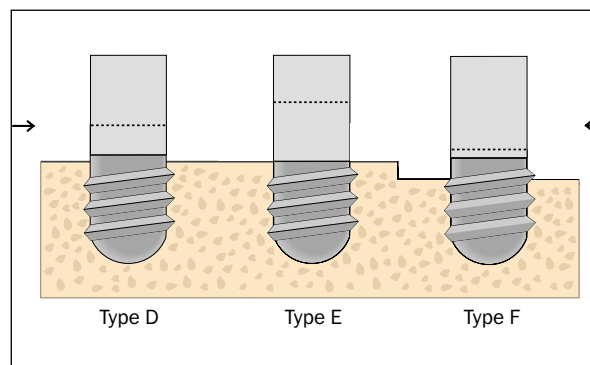
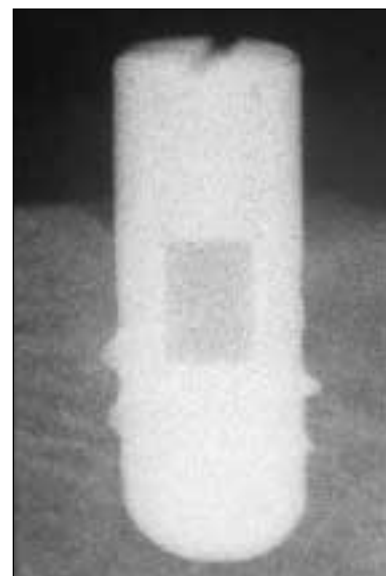


**Fig 7b** Histometric results: schematic (true to scale) of hard tissues around submerged implants types D to F at time of sacrifice in relation to the rough/smooth border (solid black line) as well as the location of the microgap/interface (dashed black line). Arrows indicate the level of the crest of the bone at the time of implant placement.

**Fig 8a** (Left) Overview of a mesiodistal histologic section (left = distal) of a type A implant (1-piece, nonsubmerged) with original inner/outer implant diameter = 3.5 mm/4.1 mm. The original cover screw was removed and replaced with a smaller-diameter transocclusal screw to facilitate histologic processing (toluidine blue and basic fuchsin stain; original magnification  $\times 2.5$ ). Bar = 1.0 mm.



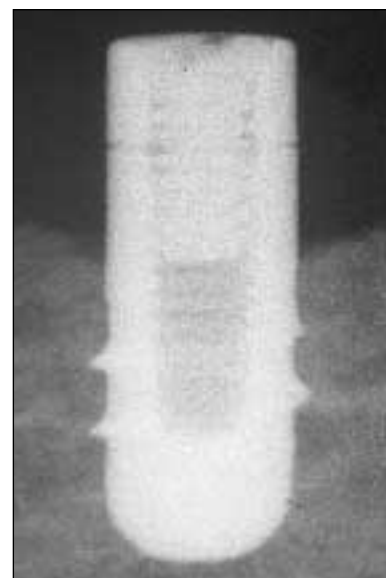
**Fig 8b** (Right) Detail of a standardized radiograph (left = distal) of the identical site shown in Fig 8a at the exact same time point (sacrifice).



**Fig 9a** (Left) Overview of a mesiodistal histologic section (left = mesial) of a type E implant (2-piece, submerged) with original inner/outer implant diameter = 3.5 mm/4.1 mm. Note that the relatively short abutment is missing because of histologic processing; however, the transocclusal abutment screw is still in place (toluidine blue and basic fuchsin stain; original magnification  $\times 2.5$ ). Bar = 1.0 mm.



**Fig 9b** (Right) Detail of a standardized radiograph (left = mesial) of the identical site shown in Fig 9a at the exact same time point (sacrifice).



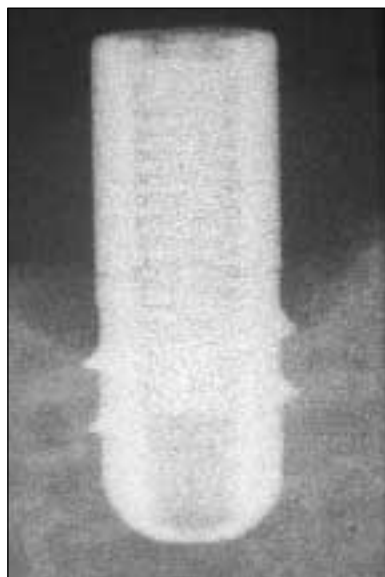


**Fig 10a** (Left) Overview of a mesiodistal histologic section (left = mesial) of a type F implant (2-piece, submerged) with original inner/outer implant diameter = 3.5 mm/4.1 mm. Note that the relatively long abutment is missing because of histologic processing; however, the transocclusal abutment screw is still in place (toluidine blue and basic fuchsin stain; original magnification  $\times 2.5$ ). Bar = 1.0 mm.

**Fig 10b** (Right) Detail of a standardized radiograph (left = mesial) of the site shown in Fig 10a at the exact same time point (sacrifice).

**Table 1 Radiographic and Histometric Data (in mm) for the 3 Different Nonsubmerged Implant Groups A to C for Top-fBIC**

Variables	Group A implants (n)	Group B implants (n)	Group C implants (n)
Radiography (mesial)	3.16 $\pm$ 0.50 (9)	3.83 $\pm$ 0.42 (10)	4.76 $\pm$ 0.24 (9)
Histometry (mesial)	3.16 $\pm$ 0.50 (9)	3.79 $\pm$ 0.40 (10)	4.72 $\pm$ 0.26 (9)
Radiography (distal)	3.02 $\pm$ 0.25 (8)	3.93 $\pm$ 0.21 (10)	4.66 $\pm$ 0.19 (9)
Histometry (distal)	2.98 $\pm$ 0.23 (8)	3.94 $\pm$ 0.19 (10)	4.62 $\pm$ 0.19 (9)

Mean values  $\pm$  standard deviations; n = number of measured implant sites.

Top-fBIC = Distance from the top of the implant to the first bone-to-implant contact.

**Table 2 Radiographic and Histometric Data (in mm) for the 3 Different Submerged Implant Groups D to F for Top-fBIC**

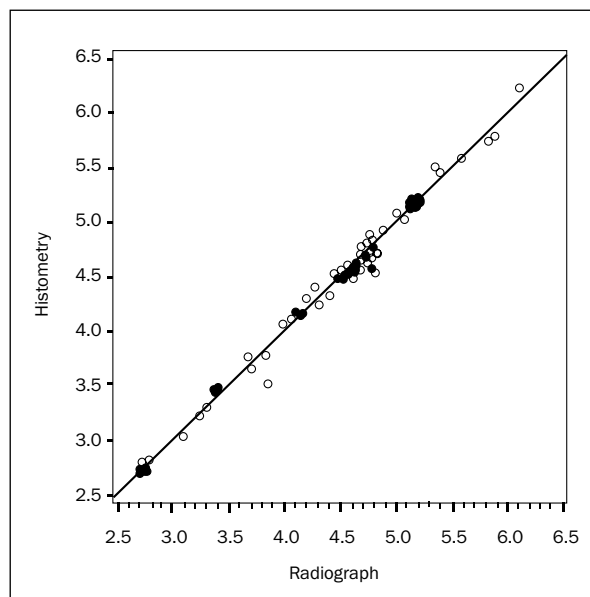
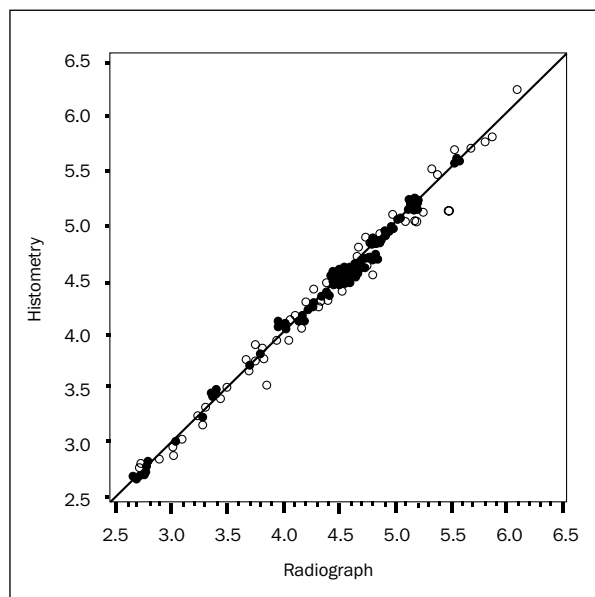
Variables	Group D implants (n)	Group E implants (n)	Group F implants (n)
Radiography (mesial)	4.60 $\pm$ 0.29 (10)	4.67 $\pm$ 0.34 (9)	5.40 $\pm$ 0.47 (10)
Histometry (mesial)	4.60 $\pm$ 0.29 (10)	4.70 $\pm$ 0.30 (9)	5.43 $\pm$ 0.46 (10)
Radiography (distal)	4.58 $\pm$ 0.20 (10)	4.73 $\pm$ 0.27 (9)	5.18 $\pm$ 0.42 (10)
Histometry (distal)	4.57 $\pm$ 0.19 (10)	4.68 $\pm$ 0.26 (9)	5.12 $\pm$ 0.44 (10)

Mean values  $\pm$  standard deviations; n = number of measured implant sites.

Top-fBIC = Distance from the top of the implant to the first bone-to-implant contact.

histometry (Figs 11a to 11c). If the Pearson correlation coefficient was significant ( $P < .01$ ) and the regression line obtained using the method of least-squares had a slope estimate not different from 1 and an intercept estimate not different from 0 by the Student  $t$  test ( $P > .10$ ), then the distances measured using standardized radiographs can be used to approximate the distances observed using histologies. This analysis was carried out for all sites together, as well as for mesial and distal sites separately.

Comparisons using paired Student  $t$  tests were made between mesial and distal sites within implant types to ascertain differences in the dimension Top-fBIC. Analyses of variance were performed to check for differences among implant types, dog, and positions in the arch. An unpaired Student  $t$  test was used to compare the left with the right side of the mandible. For all testing, probabilities less than .05 were considered significant.

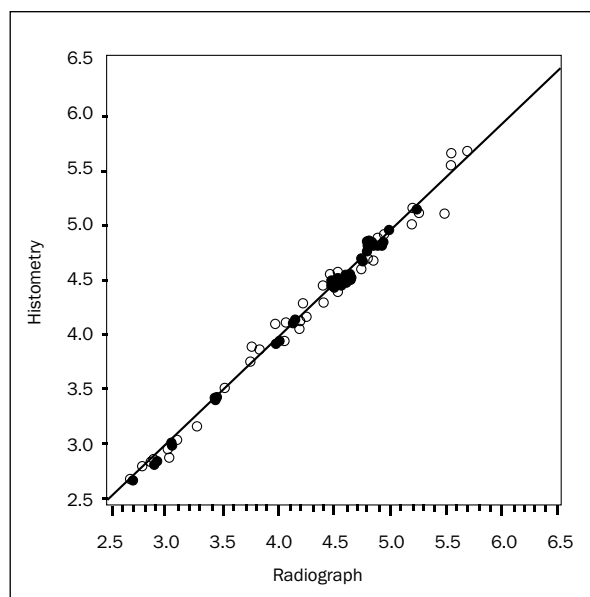


**Figs 11a to 11c** Scatter plots of the histometric data (mm) compared to the radiographic results (mm) for (left) all sites, (right) mesial sites, and (below right) distal sites.

## RESULTS

### Clinical Data

Fifty-nine of the possible 60 implants could be placed. One implant could not be placed because of anatomic limitations, since the bone at this particular site was too soft and, therefore, primary stability could not be achieved. Healing occurred without any complications after implant placement in all animals. At the time of abutment connection, 3 months after implant placement (Fig 2), all 59 implants showed successful hard tissue integration exhibiting ankylotic stability. No continuous peri-implant radiolucencies were apparent on the radiographs for all implants, as reported elsewhere.<sup>4</sup> Therefore, all 30 abutments of the submerged implant types D through F could be connected. After second-stage surgery, all implants maintained ankylotic stability and demonstrated a complication-free follow-up period. Type A and B implants (1-piece, nonsubmerged) showed no clinical symptoms of peri-implant inflammation. However, type C implants (2-piece, nonsubmerged) showed moderate to severe signs of peri-implantitis at the crestal part of the implants. Although meticulous chemical and mechanical plaque control was carried out 3 times per week, different degrees of peri-implant inflammation were detected until sacrifice for all 2-piece implants (types C through F). Around types C through F implants, this response ranged from moderate inflammation to severely inflamed peri-implant tissue that was hyperplastic in nature. These



results will be described in detail in another clinical/histomorphometric article based on this data set.

### Statistical Data

When all 113 sites were evaluated together (Tables 1 and 2; Figs 11a to 11c), the resulting Pearson correlation coefficient was 0.993 ( $P < .001$ ), and the regression line had a slope estimate of  $0.993 \pm 0.011$  (standard error) ( $P > .90$ ) and an intercept estimate

of  $0.013 \pm 0.051$  ( $P > .80$ ). This suggests that the two methods were approximately equal. In fact, 83 sites (73.4%) had a radiographic Top-fBIC distance that was within 0.1 mm of the value obtained histometrically. In 18 sites (15.9%), the measurements for standardized radiography were between 0.1 mm and 0.2 mm smaller than for nondecalcified histometry, and in 9 sites (8.0%), values for standardized radiography were between 0.1 mm and 0.2 mm larger than for the histometry. Only 3 sites (2.7%) differed by more than 0.2 mm. Each of these 3 was smaller for the standardized radiography than for the histometry, with a maximum difference of 0.38 mm.

Similar results were obtained when mesial and distal sites were analyzed separately. For the 57 mesial sites (Fig 11b), the resulting Pearson correlation coefficient was 0.994 ( $P < .001$ ), and the regression line had a slope estimate of  $1.001 \pm 0.015$  ( $P > .90$ ) and an intercept estimate of  $-0.008 \pm 0.069$  ( $P > .90$ ). Forty-four of the 57 mesial sites (77.2%) had a radiographic Top-fBIC dimension that was within 0.1 mm of the histometric value. Five sites (8.8%) were between 0.1 mm and 0.2 mm lower for the standardized radiographs, while 6 sites (10.5%) were between 0.1 mm and 0.2 mm lower for the histometry. Two sites (3.5%) were more than 0.2 mm lower for the standardized radiographs than the histometry, with a maximum difference of 0.34 mm.

For the 56 distal sites (Fig 11c), the resulting Pearson correlation coefficient was 0.992 ( $P < .001$ ), and the regression line had a slope estimate of  $0.983 \pm 0.017$  ( $P > .40$ ) and an intercept estimate of  $0.046 \pm 0.074$  ( $P > .50$ ). Thirty-nine of the 56 distal sites (69.6%) had a radiographic Top-fBIC dimension that was within 0.1 mm of the histometric value. Thirteen sites (23.2%) were between 0.1 mm and 0.2 mm lower for the standardized radiographs, while 3 sites (5.4%) were between 0.1 mm and 0.2 mm lower for the histometry. One site (1.8%) was 0.38 mm lower for the radiographs than the histometry.

For each combination of mesial and distal sites and standardized radiographic and histometric methods, the F test comparing Top-fBIC dimensions across implant types was highly significant ( $P < .001$ ). The F tests for the comparisons among dogs ( $P > .50$ ) and positions in the arch ( $P > .80$ ) indicated no significant differences. Left and right sides of the mandible were also not significantly different ( $P > .70$ ).

## DISCUSSION

In this study, endosseous titanium implants were randomly placed in a side-by-side comparison

according to a nonsubmerged or a submerged technique and in 1- or 2-piece configurations. The radiographic<sup>4</sup> and histometric results<sup>5</sup> demonstrated that a rough/smooth border on the surface of 1-piece, nonsubmerged implants determines the crestal bone level adjacent to such implants. However, in all 2-piece implants, which exhibited a microgap (interface) between the implant and the secondary component (abutment) at different levels in relation to the crest of the bone, distinct crestal bone resorption occurred around these implants. This was independent of whether 2-piece implants were placed according to a nonsubmerged or a submerged technique. Overall, submerged implants placed with their top (microgap/interface) below the alveolar crest experienced the greatest amount of crestal bone loss. Furthermore, the crestal bone resorption took place rapidly and without loading of the implants at an early time point of healing.

The purpose of the present study was to compare evaluations of crestal bone loss patterns around endosseous implants as determined by standardized linear radiography with evaluations made directly on nondecalcified histologies. Histometry of soft and hard tissues around implants can be carried out with high precision ( $\pm 0.2$  mm)<sup>5,7,13</sup> if nondecalcified histology of the bone and implant is used.<sup>19</sup> This technique permits a direct and precise identification of soft and hard tissue reference points in relation to visible, definite landmarks on an implant (eg, a microgap/interface). With a decalcified "fracture technique,"<sup>20</sup> however, in which the implant is removed, only the outline of an implant but not the implant itself can be identified on the histology.<sup>21-26</sup> Another invasive technique to determine crestal bone levels is a re-entry clinical procedure wherein a full-thickness flap is reflected prior to and after completion of an experiment<sup>27,28</sup> to allow direct measurements of crestal bone levels with a periodontal probe. However, Toback and coworkers<sup>18</sup> recently showed that the precision of this method does not come close to that of evaluations made from nondecalcified histologies, as described above.<sup>5,7,13</sup> Thus, histometry serves as a "gold standard," representing the most accurate assessment of the crestal bone level.

Histometry can only be performed if block sections can be taken from humans or animals, or if animals are sacrificed at the completion of an experiment. The cost/benefit ratio in these situations is high and often unfeasible. Periapical radiography, as a noninvasive technique, only allows examination of crestal bone levels precisely at mesial and distal sites of an implant if proper projection geometry is applied.<sup>29-34</sup> Such precision

cannot be achieved if a bisecting-angle geometry technique is used.<sup>8</sup> With the advent of the right-angle technique,<sup>9,10</sup> the paralleling technique,<sup>11</sup> and customized occlusal records combined with a long-cone technique,<sup>35</sup> projection errors related to rotation and angulation can be significantly decreased. In this study, all of the above-mentioned aspects were carefully controlled. In addition, a new rigid connection of the long cone with the beam-aiming device, as well as a firm fixation of the radiographic template to the dog's mandible during exposure, was introduced. This resulted in a modified, new technique for standardized periapical radiography in the canine.

If the outcome of standardized periapical radiography is compared to that of nondecalcified histometry, histologic sections must be available in a mesiodistal<sup>13,26,36</sup> but not in an orofacial direction.<sup>15,16,37,38</sup> This allows for direct comparison of the radiographs to the histology of identical sites. The importance of such an approach has been supported by recent findings, which showed that crestal bone loss patterns at buccal sites were significantly different from those at the mesial, lingual, and distal sites.<sup>7</sup> A direct comparison of standardized periapical radiography with nondecalcified histology was reported by Gotfredsen and coworkers<sup>13</sup> using a combination of orofacial and mesiodistal sections. In their material, a positive correlation between mesiodistal and orofacial histometric values was found, with relatively low correlation coefficients of  $r = 0.67$  (buccal versus mesiodistal sites) and  $r = 0.73$  (lingual versus mesiodistal sites). This might be a result of the fact that buccal sites seem to have different crestal bone loss patterns, as already described above.<sup>5,7</sup> In the study by Gotfredsen and coworkers,<sup>13</sup> a significantly high correlation ( $P < .001$ ) was found for the overall comparison of standardized periapical radiography with nondecalcified histology, with a correlation coefficient of  $r = 0.94$ . These numbers were improved in the present study utilizing a modified radiographic technique, with a correlation coefficient of  $r = 0.99$  ( $P < .001$ ). This supports the fact that highly standardized radiographs allow for accurate evaluation of crestal bone levels in these experimental animal models.

Both histometric as well as radiographic measurements in the canine mandible have been carried out with high precision of up to 0.01 mm, resulting in a correlation coefficient of  $r = 0.99$  ( $P < .001$ ) when these techniques are compared with each other, as related to above-mentioned data from other animal studies. This supports the fact that, when taking periapical radiographs in humans, an attempt should be made to perfectly align the radio-

graphic film with the long axis of the implant to evaluate crestal bone loss patterns (right-angle technique combined with paralleling technique and a customized bite record). Even though it might not be possible to apply such a template design in humans using appropriate attachments, a technique similar to that suggested first by Benkow<sup>9,10</sup> should allow the achievement of similar precision of some 0.1 mm, which, in a clinical setting, still would permit clinicians to distinguish healthy peri-implant conditions from pathologic peri-implant crestal bone resorption.

Several authors have reported that the results of periapical radiography, with respect to the degree of crestal bone loss, underestimated the results of histometric analyses.<sup>13-16,18,36</sup> One reason for this phenomenon might be that even though a right-angle technique was used in those studies, a parallel orientation of the bite block (film plane) to the long axis of the tooth (parallel technique) could not always be achieved. This happens most often in the maxilla because of the strong inclination of the palate and/or a low palate. Another reason might be the fact that periapical radiographic data show in a cumulative way the whole width of the jaw, making it more difficult to identify fBIC as a result of superimposition, with calcified structures of the jaw itself resulting in a distinct underestimation of the degree of crestal bone loss. This problem does not occur when evaluating histologic specimens, since the width of the sections ranges between 10 and 80  $\mu\text{m}$ , thereby allowing detection of only bone that is in direct contact to the implant. Thus, the evaluation of radiographs has more potential error than the analysis of histologic specimens.

## CONCLUSION

It can be noted that this modified clinical laboratory technique for standardized periapical radiography in the canine model allows for a highly precise evaluation of mesial and distal peri-implant crestal bone levels. This finding is significant because of the fact that crestal bone levels can be determined using a noninvasive technique (standardized radiography, as described above), and block sectioning or sacrifice of experimental animals is not required. In addition, longitudinal evaluations can be made accurately such that precise bone changes can be assessed over various time periods. Such evaluations may prove beneficial in clinicians' attempts to distinguish physiologic changes from pathology or determine the cause and effect of bone changes around dental implants.

## ACKNOWLEDGMENTS

The authors would like to thank Sonja A. Bustamante, HT (ASCP), University of Texas Health Science Center at San Antonio (UTHSCSA), for her continuous and valuable support throughout the study. Richard J. Haines, DVM, Clinical Veterinarian, and his team, Laboratory Animal Resources, UTHSCSA, are greatly acknowledged for exemplary care of the animals. In addition, the authors would like to express their gratitude to James P. Simpson, BSc (Eng), PhD, and Institut Straumann AG, Waldenburg, Switzerland, for manufacturing the test implants. Last but not least, we would like to express our appreciation for the outstanding work by Britt Hoffmann, HT, University of Bern School of Dental Medicine, in preparing the histologic sections. This study has been supported by two grants from the ITI (International Team for Oral Implantology) Foundation for the Promotion of Oral Implantology (#02-94/061, #20-97/134), Waldenburg, Switzerland; and by stipends from the Swiss National Science Foundation, Basel, Switzerland; the Swiss Society of Periodontology, Bern, Switzerland; the Swiss Foundation for Medical and Biological Stipends, Bern, Switzerland; and the University of Basel Committee for the Promotion of *Philosophiae Doctor* Candidates, Basel, Switzerland.

## REFERENCES

- Younger WJ. Pyorrhea alveolaris in the times of the pharaohs and the present Egyptians. *Am Dent Soc Eur Trans* 1905;85-89.
- Ericsson I, Berglundh T, Marinello C, Liljenberg B, Lindhe J. Long-standing plaque and gingivitis at implants and teeth in the dog. *Clin Oral Implants Res* 1992;3:99-103.
- Cochran DL, Hermann JS, Schenk RK, Higginbottom FL, Buser D. Biologic width around titanium implants. A histometric analysis of the implant-gingival junction around unloaded and loaded nonsubmerged implants in the canine mandible. *J Periodontol* 1997;68:186-198.
- Hermann JS, Cochran DL, Nummikoski PV, Buser D. Crestal bone changes around titanium implants. A radiographic evaluation of unloaded nonsubmerged and submerged implants in the canine mandible. *J Periodontol* 1997;68:1117-1130.
- Hermann JS, Buser D, Schenk RK, Cochran DL. Crestal bone changes around titanium implants. A histometric evaluation of unloaded nonsubmerged and submerged implants in the canine mandible. *J Periodontol* 2000;71:1412-1424.
- Hermann JS, Buser D, Schenk RK, Higginbottom FL, Cochran DL. Biologic width around titanium implants. A physiologically formed and stable dimension over time. *Clin Oral Implants Res* 2000;11:1-11.
- Hermann JS, Buser D, Schenk RK, Schoolfield JD, Cochran DL. Biologic width around one- and two-piece titanium implants. A histometric evaluation of unloaded nonsubmerged and submerged implants in the canine mandible. *Clin Oral Implants Res* (in press).
- Price WA. The technique necessary for making good dental skiagraphs. *Items Interest* 1904;26:161-171.
- Benkow HH. Periodisk-identiske og stereoskopiske introrale røntgenopptak. *Den Norske Tannlaege Tidende* 1956;66:239-255.
- Benkow HH. A new principle for clinical roentgenographic tooth measurement. *Odontol Tidsk* 1960;68:423-449.
- Rosling B, Hollender L, Nyman S, Olsson G. A radiographic method for assessing changes in alveolar bone height following periodontal therapy. *J Clin Periodontol* 1975;2:211-217.
- Larheim TA, Eggen S. Measurements of alveolar bone height at tooth and implant abutments on intraoral radiographs. A comparison of reproducibility of Eggen technique utilized with and without a bite impression. *J Clin Periodontol* 1982;9:184-192.
- Gotfredsen K, Rostrup E, Hjørting-Hansen E, Stoltze K, Budtz-Jørgensen E. Histological and histomorphometrical evaluation of tissue reactions adjacent to endosteal implants in monkeys. *Clin Oral Implants Res* 1991;2:30-37.
- Tonetti MS, Pini Prato G, Williams RC, Cortellini P. Periodontal regeneration of human infrabony defects. III. Diagnostic strategies to detect bone gain. *J Periodontol* 1993;64:269-277.
- Evans GH, Mendez AJ, Caudill RF. Loaded and nonloaded titanium versus hydroxyapatite-coated threaded implants in the canine mandible. *Int J Oral Maxillofac Implants* 1996;11:360-371.
- Caulier H, Naert I, Kalk W, Jansen JA. The relationship of some histologic parameters, radiographic evaluations, and Periotest measurements of oral implants: An experimental animal study. *Int J Oral Maxillofac Implants* 1997;12:380-386.
- Isidor F. Mobility assessment with the Periotest system in relation to histologic findings of oral implants. *Int J Oral Maxillofac Implants* 1998;13:377-383.
- Toback G, Brunsvold MA, Nummikoski PV, Masters LB, Mellonig JT, Cochran DL. The accuracy of radiographic methods in assessing the outcome of periodontal regenerative therapy. *J Periodontol* 1999;70:1479-1489.
- Schenk RK, Olah AJ, Herrmann W. Preparation of calcified tissues for light microscopy. In: Dickson GR (ed). *Methods of Calcified Tissue Preparation*. Amsterdam: Elsevier, 1984:1-56.
- Thomsen P, Ericson LE. Light and transmission electron microscopy used to study the tissue morphology close to implants. *Biomaterials* 1985;6:421-424.
- Berglundh T, Lindhe J, Ericsson I, Marinello CP, Liljenberg B, Thomsen P. The soft tissue barrier at implants and teeth. *Clin Oral Implants Res* 1991;2:81-90.
- Berglundh T, Lindhe J, Marinello C, Ericsson I, Liljenberg B. Soft tissue reaction to de novo plaque formation on implants and teeth. An experimental study in the dog. *Clin Oral Implants Res* 1992;3:1-8.
- Abrahamsson I, Berglundh T, Wennström J, Lindhe J. The peri-implant hard and soft tissues at different implant systems. A comparative study in the dog. *Clin Oral Implants Res* 1996;7:212-219.
- Berglundh T, Lindhe J. Dimension of the periimplant mucosa. Biological width revisited. *J Clin Periodontol* 1996;23:971-973.
- Abrahamsson I, Berglundh T, Lindhe J. The mucosal barrier following abutment dis/reconnection. An experimental study in dogs. *J Clin Periodontol* 1997;24:568-572.
- Abrahamsson I, Berglundh T, Moon IS, Lindhe J. Peri-implant tissues at submerged and non-submerged titanium implants. *J Clin Periodontol* 1999;26:600-607.
- Langer B, Gelb DA. The early reentry procedure. *J Periodontol* 1977;48:318-324.
- Langer B, Gelb DA, Krutchkoff DJ. Early re-entry procedure. Part II. A five year histologic evaluation. *J Periodontol* 1981;52:135-139.

29. Sewerin IP. Errors in radiographic assessment of marginal bone height around osseointegrated implants. *Scand J Dent Res* 1990;98:428–433.
30. Sewerin IP. Estimation of angulation of Brånemark titanium fixtures from radiographic thread images. *Clin Oral Implants Res* 1991;2:20–23.
31. Sewerin I. Radiographic image characteristics of Brånemark titanium fixtures. *Swed Dent J* 1992;16:7–12.
32. Gher ME, Richardson AC. The accuracy of dental radiographic techniques used for evaluation of implant fixture placement. *Int J Periodontics Restorative Dent* 1995;15:268–283.
33. Sewerin IP, Gotfredsen K, Stoltze K. Accuracy of radiographic diagnosis of peri-implant radiolucencies—An in vitro experiment. *Clin Oral Implants Res* 1997;8:299–304.
34. Begoña Ormaechea M, Millstein P, Hirayama H. Tube angulation effect on radiographic analysis of the implant-abutment interface. *Int J Oral Maxillofac Implants* 1999;14:77–85.
35. Larheim TA, Wie H, Tveito L, Eggen S. Method for radiographic assessment of alveolar bone level at endosseous implants and abutment teeth. *Scand J Dent Res* 1979;87:146–154.
36. Isidor F. Clinical probing and radiographic assessment in relation to the histologic bone level at oral implants in monkeys. *Clin Oral Implants Res* 1997;8:255–264.
37. Hürzeler MB, Quiñones CR, Schüpbach P, Vlassis JM, Strub JR, Caffesse RG. Influence of the suprastructure on the peri-implant tissues in beagle dogs. *Clin Oral Implants Res* 1995;6:139–148.
38. Levy D, Deporter DA, Pilliar RM, Watson PA, Valiquette N. Initial healing in the dog of submerged versus non-submerged porous-coated endosseous dental implants. *Clin Oral Implants Res* 1996;7:101–110.